

# Numerical Investigation of Magnetic Nanoparticles Trajectories for Magnetic Drug Targeting

Syireen Shazri and Moumen Idres

Mechanical Engineering Department, Kuliyah of Engineering, International Islamic University Malaysia, 50728 Kuala Lumpur, Malaysia

midres@iiu.edu.my

**Abstract.** In this work, the trajectories and capturing of magnetic nanoparticles coated with drug agent are investigated for drug targeting application. Nanoparticles are injected at the entrance of a microvessel and captured by a permanent magnet located at a specified location where tumor exists. The problem is divided into two steps; blood flow solution and nanoparticles trajectory solution. The blood flow in microvessel is obtained both analytically and numerically. Integration of nanoparticles equations of motion to obtain the trajectories is performed using both Matlab and ANSYS Fluent. Discrete Phase Model (DPM) in ANSYS Fluent is used for nanoparticles tracking. The dominant magnetization and drag forces acting on magnetic particles are incorporated to study the trajectories of magnetic particles. Parametric studies for steady flow with single point and multiple point injections are conducted. This includes varying particle diameter and magnet location. Critical minimum diameter for capturing is predicted. Capturing efficiency is reported for all cases. It is found that particle trajectories are strongly dependent on particle size and location of the magnet. The simulation can be used to determine the optimum particle size for treating a tumor, given its size and location.

## 1. Introduction

Magnetic Drug Targeting (MDT) provides a promising technique for improving the available conventional drug delivery techniques. During chemotherapy, for example, the drug is not only concentrated locally on the tumor tissue, but it is globally exposed to the other healthy tissues throughout the body. To avoid damages to healthy cells from the toxic drug, it is highly recommended to physically target the drug to the specific locations where the unhealthy cells exist. In MDT technique, ferrofluids consisting of suspended magnetic nanoparticles are used as a carrier for chemotherapeutic agents and for other medications. Then, they are targeted to a specified location by the help of an applied magnetic field coming from an external permanent magnet. The role of the external magnet is to provide the magnetic force that can attract and capture the magnetic particles. This allows the treatment to be targeted locally to the only necessary locations instead of going globally throughout the body, which can cause side effects. This technique can be very useful for treating many diseases such as cancer, stenosis, arterial occlusion, stroke, and much more.

The use of ferrofluids for magnetic drug targeting has become the primary carriers due to their high saturation magnetization and magnetic susceptibility. For general applications, ferrofluids in pharmaceutical and medical applications should be biocompatible, biodegradable, and nontoxic [1].



Magnetite nanoparticles ( $\text{Fe}_3\text{O}_4$ ) that have excellent magnetic saturation ( $\sim 78$  emu/g) are desirable for these applications due to the strong ferromagnetic behavior, less sensitivity to oxidation and relatively low toxicity compared to many other materials (e.g., nickel and cobalt) [2]. Such nanoparticles can be driven to the specific target site by applying external magnetic fields. The effectiveness of this technique is critically dependent on the properties of magnetic nanoparticles [3-5]. Ferrofluids are also dielectric (non conducting) and paramagnetic which means they are attracted by magnetic fields, and do not retain magnetization in the absence of an applied field [6].

There are many recent studies regarding this magnetic drug targeting technique. Furlani et al., 2009 presented an analytic model for transport and capture of magnetic nanoparticles in the human microvasculature for targeted drug delivery applications [7]. He also performed parametric studies by varying the size of magnetic particles and the distance of the external magnetic field. It is also been reported that the magnetic drug targeting is relatively safe and effective for targeting the drugs to a desired and specific location in patient's body [8-9]. Micron sized magnetic particles have been injected in a capillary of a blood vessel inside a tumor by locating an external magnetic field by 10 cm away from the tumor location [10].

During targeting, not all the particles will be trapped since part of them will be lost between the injection and the target point. The efficiency of the target and capture of the magnetic nanoparticles is very important in order to have a maximum-trapped drug in the desired location. Thus, it is vital to study about the optimal parameters such as magnetic nanoparticle size and external magnetic field that can significantly improve the efficiency of the magnetic drug targeting.

In this work, we presented several theoretical formulae and performed simulations through finite volume based ANSYS Fluent software under Discrete Phase Model (DPM) to predict the trajectories and captures of magnetic nanoparticles at the microvessel wall. Different magnetic particle radii and different external magnet locations are varied to observe the effect on particle trajectories. Two cases of injections are performed; single point injection and multipoint injection case. This study will help to design a better drug targeting technique with optimized size of magnetic nanoparticles and the relative location of the external magnet.

## 2. Methodology

Figure 1 depicts the schematic diagram or geometric configuration that simulated the particle trajectories in the two-dimensional straight cylindrical tube of microvessel with a radius ( $R_v$ ). A cylindrical external permanent magnet with a radius of  $R_{mag}$  is located at a distance of  $y_{mag}$  from the axis and  $x_{mag}$  from the inlet of the vessel. This cylindrical magnet with the role of producing the requisite magnetic field is assumed to be infinitely long and oriented perpendicular to the direction of the blood flow.

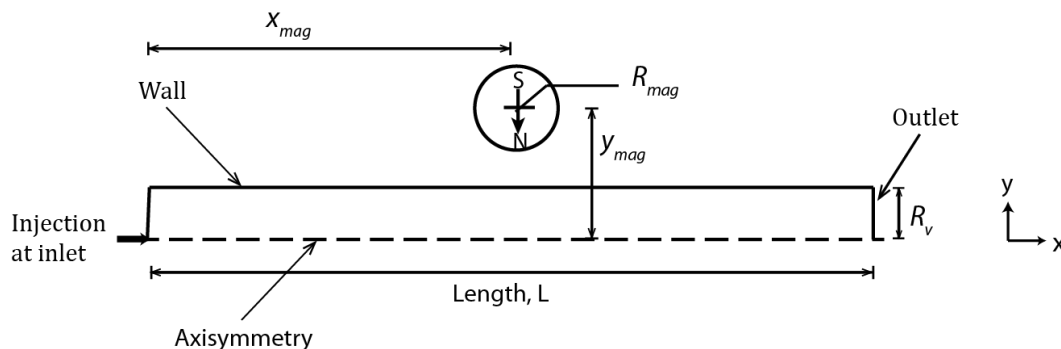


**Figure 1.** Schematic diagram for predicting particle trajectories in microvessel.

### 2.1. Theoretical Formulation

There are many forces acting simultaneously on the magnetic particles as they are transported in the microvessel. The forces are magnetic force, viscous drag force, gravitational force, and buoyancy force. The other factors that affect the motion of magnetic nanoparticle in microvessel are Brownian motion and particle inertial effect. However, in this model, only dominant forces which are the magnetic force and viscous drag force are considered, while the rest of the other forces are neglected.

The trajectory of the magnetic particles is predicted by integrating the Newton's law of equation of motion

$$m_p \frac{d\mathbf{u}_p}{dt} = \mathbf{F}_D + \mathbf{F}_m \quad (1)$$

where  $m_p$  and  $\mathbf{u}_p$  denote the mass and the velocity vector of the magnetic nanoparticle respectively, while  $\mathbf{F}_D$  and  $\mathbf{F}_m$  are the viscous drag force and magnetic force.

The viscous drag force was predicted by using spherical drag law from Stoke's approximation as following [13]

$$\mathbf{F}_D = -6\pi\eta R_p(\mathbf{u}_p - \mathbf{u}_f) \quad (2)$$

where  $R_p$  is the radius of the particle,  $\eta$  is the viscosity of the fluid,  $\mathbf{u}_p$  and  $\mathbf{u}_f$  are the velocities of the particles and fluid respectively. The flow is determined in terms of average speed of  $u_f$

$$u_f(y) = 2u_{f,average} \left(1 - \frac{y^2}{R_v^2}\right) \quad (3)$$

where  $u_f(y)$  is the velocity of fluid in the axial direction at a radial distance,  $y$  from its axis.

Next, for the magnetic force  $\mathbf{F}_m$ , which also known as the Kelvin force on a magnetized particle of volume,  $V$  is given by the following equation,

$$\mathbf{F}_m = \iiint_V \mu_0 \mathbf{M} \cdot \nabla \mathbf{H} dV \quad (4)$$

Where  $\mu_0 = 4\pi \times 10^{-7} \text{N/A}^2$  is the magnetic permeability of vacuum,  $\mathbf{M}$  is the material's magnetization (magnetic dipole moment per unit volume), and  $\mathbf{H}$  is the auxiliary magnetic field vector.

Furthermore, to determine the magnetic force, a model for the magnetic response of the particle is needed. We considered the particles are below saturation and the magnetization of such particles can often be assumed proportional to the applied magnetic field. In other words, we used a linear magnetization model with saturation.

$$\mathbf{M} = \chi \mathbf{H} \quad (5)$$

Here the proportionality constant  $\chi$  is called the magnetic susceptibility. The magnetic susceptibility  $\chi$  quantifies the tendency of a material to form magnetic dipoles. The effective susceptibility of the spherical particles is related to their intrinsic susceptibility. Since we have assumed the particle is below saturation, the intrinsic susceptibility,  $\chi_{eff} = 3$ .

After the integration of equation (4), the magnetic force term due to the presence of the magnetic field is expressed as following,

$$\mathbf{F}_m = \mu_0 \left(\frac{4}{3}\pi R_p^3\right) \chi_{eff} (\mathbf{H} \cdot \nabla) \mathbf{H} \quad (6)$$

The magnetic field in the expression of the coordinate reference frame of the microvessel is derived by the following equations,

$$\mathbf{H} = H_x(x, y)\hat{\mathbf{x}} + H_y(x, y)\hat{\mathbf{y}} \quad (7)$$

Next, the magnetic field terms in equation (6) is reduced to the following equation,

$$\nabla H_a^2 = H_x(x, y) \frac{\partial H_x(x, y)}{\partial y} + H_y(x, y) \frac{\partial H_y(x, y)}{\partial y} \quad (8)$$

This can be reduced after we have assumed  $\mathbf{rot} \mathbf{H} = 0$ . This results in  $\frac{\partial H_x(x, y)}{\partial y} = \frac{\partial H_y(x, y)}{\partial x}$  and finally leads to this expression;  $(\mathbf{H} \cdot \nabla)\mathbf{H} = \nabla H_a^2$ .

The magnetic force in equation (6) can also be written in the  $x$ - and  $y$ -component as in the following equation,

$$\mathbf{F}_m(x, y) = F_{mx}(x, y)\hat{\mathbf{x}} + F_{my}(x, y)\hat{\mathbf{y}} \quad (9)$$

Substitute equation (8) into equation (6) in the form of equation (9),

$$F_{mx}(x, y) = \mu_0 \left( \frac{4}{3} \pi R_p^3 \right) \chi_{eff} \left[ H_x(x, y) \frac{\partial y(x, y)}{\partial x} + H_y(x, y) \frac{\partial H_y(x, y)}{\partial y} \right] \quad (10)$$

$$F_{my}(x, y) = \mu_0 \left( \frac{4}{3} \pi R_p^3 \right) \chi_{eff} \left[ H_x(x, y) \frac{\partial H_x(x, y)}{\partial x} + H_y(x, y) \frac{\partial H_x(x, y)}{\partial y} \right] \quad (11)$$

Next, the external source magnet at the horizontal distance,  $x_{mag}$  and vertical distance,  $y_{mag}$  with a radius of  $R_{mag}$  (centered at its local origin) as shown in figure 1 is considered in the formulation of the magnetic force. The magnetization of the source magnet is assumed to be at a level of  $M_s = 1 \times 10^6 \text{ A/m}$  through its cross section. Then, the final form of magnetic force can be written as the following,

$$F_{mx}(x, y) = -\mu_0 \left( \frac{4}{3} \pi R_p^3 \right) \chi_{eff} M_s^2 R_{mag}^4 \frac{x - x_{mag}}{2[(y - y_{mag})^2 + (x - x_{mag})^2]^3} \quad (12)$$

$$F_{my}(x, y) = -\mu_0 \left( \frac{4}{3} \pi R_p^3 \right) \chi_{eff} M_s^2 R_{mag}^4 \frac{y - y_{mag}}{2[(y - y_{mag})^2 + (x - x_{mag})^2]^3} \quad (13)$$

Lastly, the equation of motion shown in equation (1) is then written in its final form that comprises of  $x$ - and  $y$ -component as stated in the following equation (14) and (15). These two equations are also been used to make a comparison between the analytical and the numerical solutions (from Fluent) for single injection point. Meanwhile, equation (16) shows the formula for determining the capture efficiency in multipoint injection case.

$$m_p \frac{du_{px}}{dt} = -\mu_0 \left( \frac{4}{3} \pi R_p^3 \right) \chi_{eff} M_s^2 R_{mag}^4 \frac{x - x_{mag}}{2[(y - y_{mag})^2 + (x - x_{mag})^2]^3} - 6\pi\eta R_p \left[ u_{px} - 2u_f \left( 1 - \frac{y^2}{R_v^2} \right) \right] \quad (14)$$

$$m_p \frac{du_{py}}{dt} = -\mu_0 \left( \frac{4}{3} \pi R_p^3 \right) \chi_{eff} M_s^2 R_{mag}^4 \frac{y - y_{mag}}{2[(y - y_{mag})^2 + (x - x_{mag})^2]^3} - 6\pi\eta R_p u_{py} \quad (15)$$

$$\text{Capture Efficiency} = \frac{\text{Trapped particle}}{\text{Injected particle}} \quad (16)$$

## 2.2. Solution and Numerical Methods

In this work, there are two ways of solving the equations of motion of magnetic particles for predicting their trajectories. For single injection case, the trajectories of particles are predicted through simulations using ANSYS Fluent under DPM. Meanwhile, for multipoint injection case, the trajectories of the particles are predicted by solving the equations of motion analytically and numerically using Matlab.

Discrete Phase Model plays an important role in tracking particles hence the trajectories of particles can be predicted. Discrete Phase Model in ANSYS Fluent follows the Euler-Lagrange approach. The fluid phase, which is the continuous phase, is treated as a continuum by solving the time-averaged Navier-Stokes equations in the Eulerian reference frame. Meanwhile, the dispersed phase is solved by tracking the number of particles through the calculated flow field of the continuous phase in Lagrangian reference frame [11].

For continuous phase, the pressure-based solver is selected and under this, pressure-velocity coupling method with selecting SIMPLE segregated algorithm using the semi-implicit method is been done. The SIMPLE algorithm uses a relationship between velocity and pressure corrections to enforce the conservation of mass and to obtain the pressure field. The pressure corrections can be obtained by specifying the under-relaxation factor for pressure which usually around 0.03. For spatial discretization scheme, Least Square Cell-Based scheme is used to discretize the gradient, whereas central differencing scheme of second order accuracy is used to discretize the pressure and second order upwind to discretize momentum.

For discrete phase, ANSYS Fluent predicted the trajectory of a particle by integrating the force balance on the particle as in equation (1), which is written in a Lagrangian reference frame [11]. In this case, the particle is only subjected to a fluidic drag force and magnetic force as stated previously. The magnetic force in equation (12) and equation (13) are compiled into Fluent using a User Defined Function(UDF) option. They are programmed using the C language based on the particle position, not the cell position [12]. They are also being hooked in the “body force” options under DPM.

The trajectory equation is solved by stepwise integration over discrete time steps using the trapezoidal discretization scheme. The maximum number of time steps used to compute a single particle trajectory via integration of equation (1) used in the simulation is 100000. This should be large enough so that the particles can travel from entrance to exit. When the maximum number of steps is exceeded; ANSYS Fluent abandons the trajectory calculation for the current particle injection and reports the trajectory fate as “incomplete” [12]. Step Length Factor is inversely proportional to the integration time step. It is roughly equivalent to the number of time steps required to traverse the current continuous phase control volume. In this simulation, the step length factor is chosen as 5.

For single injection, a particle was released from the inlet at one point, which is exactly at the axis of the vessel. The fluid flow is assumed as laminar and axisymmetric flow with a no-slip boundary condition at the wall. For DPM boundary condition, the inlet and outlet were set to allow particles to escape while the wall of the vessel is set to trap the particles. The particle is being tracked using only for “one-way coupling” and steady particle tracking in DPM.

Next, for multipoint injection case, the prediction of magnetic particles trajectories is done by solving equation (14) and (15) analytically and numerically. Stiff Ordinary Differential Equation (ODE23s) in Matlab is used to solve the numerical parts instead of using ANSYS DPM. For this case, since the particles are injected at many different points through the inlet, the axisymmetric flow option in Fluent cannot be selected because the magnetic force is unsymmetrical across the entire domain of the microvessel. This results in the unsymmetrical particles trajectories. This is the reason for why we could not simulate the trajectories in Fluent since only the fluid flow is axisymmetric but not the particle trajectories.

Hence, in equation (14) and (15), the magnetic force terms are solved numerically using ODE23s, while the viscous drag force terms are solved analytically. From these two solutions, the particles trajectories are been predicted for the multipoint injection case.

### 2.3. Mesh Independency

Mesh independence study is very important in computational fluid dynamics to achieve a fair accurate solution. The size of mesh needs to be tested and specified for different mesh densities in order to have the best mesh independency within a reasonable CPU time. Mesh is refined until the solution is independent of the variation of the mesh size.

The range of sizes of the mesh consisting of fine, medium, and coarse sizes are varied in the radial direction (orthogonal to the flow) and in the axial direction (parallel to the flow). After the calculation is done, the convergence histories for all the meshes are plotted. Then, the accuracy of each mesh is analyzed. In order to identify which mesh has better accuracy, the velocity profile of the flow solution at the outlet of microvessel for each mesh is plotted. It is then been compared with the analytical velocity profile formula for fully developed flow as presented in equation (3).

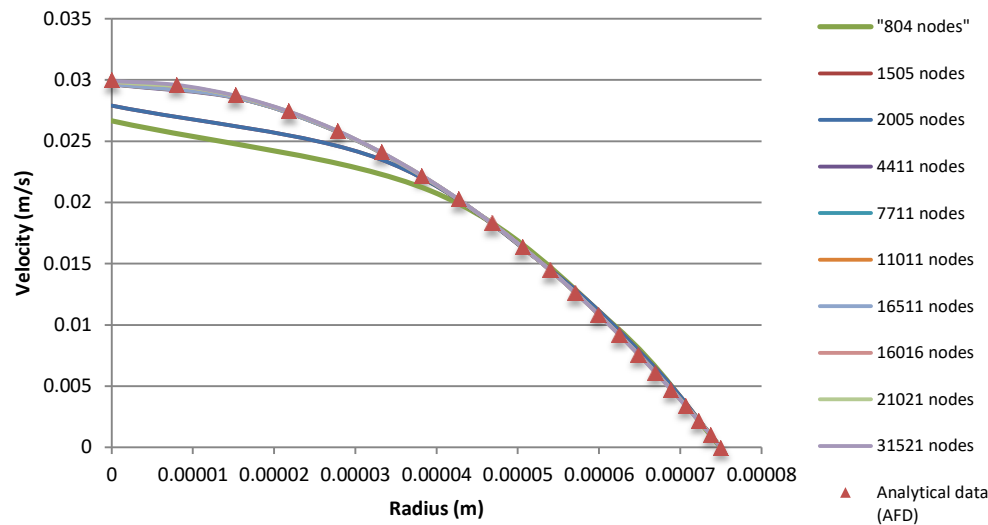
## 3. Results and Discussion

The magnetic nanoparticles with the density of  $5000 \text{ kg/m}^3$  are injected into the microvessel ( $L = 16 \text{ cm}$  and  $R_v = 75 \mu\text{m}$ ). The cylindrical external permanent magnet with a radius of  $R_{mag} = 2 \text{ cm}$  is placed at a distance of  $y_{mag}$  and  $x_{mag} = 8 \text{ cm}$ . The magnetic nanoparticles with different radii ranging from  $150 \text{ nm}$  to  $350 \text{ nm}$  are injected parallel with the same fluid flow velocity ( $x$ -direction). The flow is assumed to be a laminar artificial blood flow with the velocity,  $u_f$  of  $0.015 \text{ m/s}$ , density,  $\rho$  of  $1056 \text{ kg/m}^3$  and viscosity,  $\eta$  of  $0.0036 \text{ N s/m}^2$ .

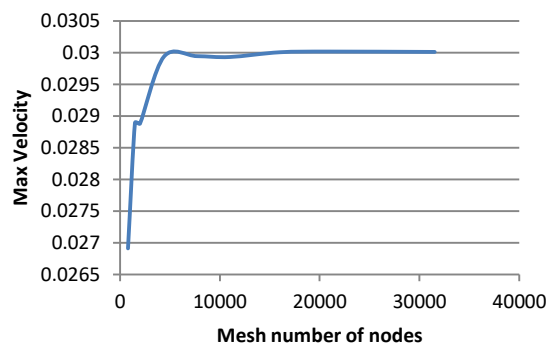
### 3.1. Mesh Independence

Figure 2 depicts 10 velocity profiles solutions from different mesh sizes. All the velocity profiles are plotted together with the analytical solution. It is observed that the higher number of nodes, which means finer mesh, has higher accuracy when compared with the analytical solution. It shows that the higher the number of nodes or elements, the smaller the error is.

However, we should also consider the time taken for CPU to solve the simulation. To that extent, we will observe at which mesh the solution will be constant and not dependent anymore on the refinement of mesh. From figure 3, the maximum velocity at the centerline of the vessel is plotted. From this figure, approximately at node number 16000, the solution started to have a constant value even though the mesh is refined more. We chose this mesh size because it is reasonable since the fully developed flow at the outlet and the error for the maximum velocity at the centerline is showing the least error when compared with the analytical data as shown in figure 4. It is also reasonable if compared to the other finest meshes as those meshes need more time to have a converged solution.



**Figure 2.** Velocity profiles at outlet for different mesh sizes.



**Figure 3.** Mesh number of nodes against the maximum velocity at centerline.

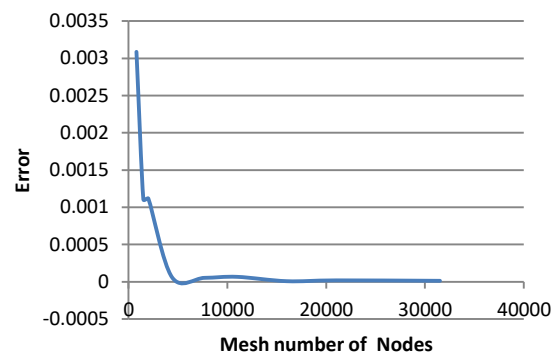


**Figure 4.** Mesh number of nodes against the error of maximum velocity with AFD.

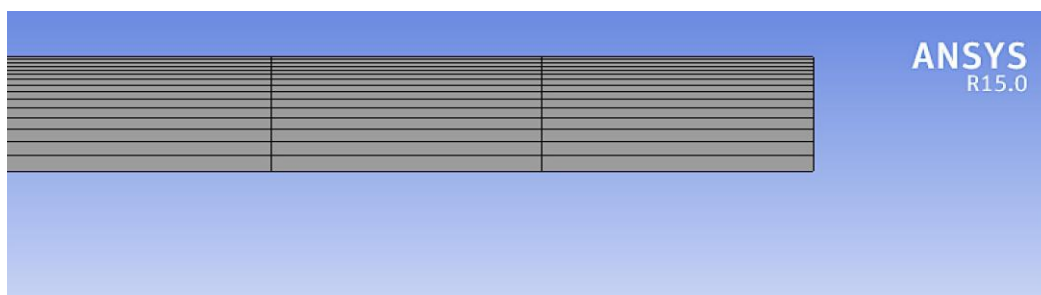


**Figure 5.** Structured non-uniform mesh.

Furthermore, in this project, the domain was discretized into a large number of quadrilateral structured meshes, which has been specified through mesh independence study. 15000 number of elements. Since the velocity is changing in the  $y$ -direction (orthogonal to the flow), thus the mesh resolution needs to be higher in that direction or in other words, the mesh size needs to be finer at the wall of the domain. In order to make it finer or higher resolution only at the wall of the domain, bias

factor of 6 is specified. Finer meshes are not recommended to be used through the entire domain since it will take longer time for solver to run. This means that the non-uniform mesh will be applied since the refinement of the mesh only recommended on the region of interest.

### 3.2. Single Point Injection Case

We predicted the trajectories of five different sizes of particles which are  $R_p = 150, 200, 250, 300, 350$  nm. These five particles are being injected at different locations of magnet-to-vessel distances which are  $y_{mag} = 0.025, 0.03, 0.035$  m as shown in Figure 1. Each particle is being injected at the origin point ( $x = 0$  and  $y = 0$ ), which is far enough upstream to have a negligible magnetic force acting on the particle during injection.

The data of each simulated particle trajectory are being exported from ANSYS Fluent to Microsoft Excel so that they can be normalized easier. The particle trajectory needs to be normalized by since the length of the domain is extremely long if compared to its radius resulting in unclear and invisible particle trajectory. Therefore, the radial position of the particle is normalized with respect to the microvessel radius ( $R_v$ ), while the axial position ( $x$ ), is normalized with respect to the magnet radius ( $R_{mag}$ ). After normalization, the  $x_{mag}$  location at the  $x$ -axis is at point 4 in figure (6), (7) and (8).

From the plots also, it can be shown that for  $y_{mag}=0.025$  m as in figure (6), only the smallest particle with a radius of 150 nm is escaped and the rest four particles are being captured at the wall of the vessel. For  $y_{mag}=0.030$  m as shown in figure (7), the particle with a radius of 150 nm and 200 nm are escaped and the rest three particles are being captured at the wall of the vessel. Lastly, for  $y_{mag}=0.035$  m in figure (8), only the largest particle is being captured and the rest four are escaped. From these, we can conclude that the magnetic force acting on the particle is directly proportional to the volume of the particle. It has been shown that fewer particles are being captured as  $y_{mag}$  is increasing. Only a larger particle experienced a stronger capture force and can be captured at a higher value of  $y_{mag}$  (farther distance).

Furthermore, the minimum capture radius particle for each of  $y_{mag}$  distance also being predicted. For  $y_{mag} = 0.025$  m, the minimum captured radius is 150 nm, for  $y_{mag} = 0.0250$  m, the minimum capture radius is 250 nm, and lastly, for  $y_{mag} = 0.035$  m, the minimum capture radius is 350 nm.

From this parametric study, it can be shown that the magnetic particle trajectories are strongly dependent on the particle size and the location of the source magnet that will give the magnetic force on the particles.



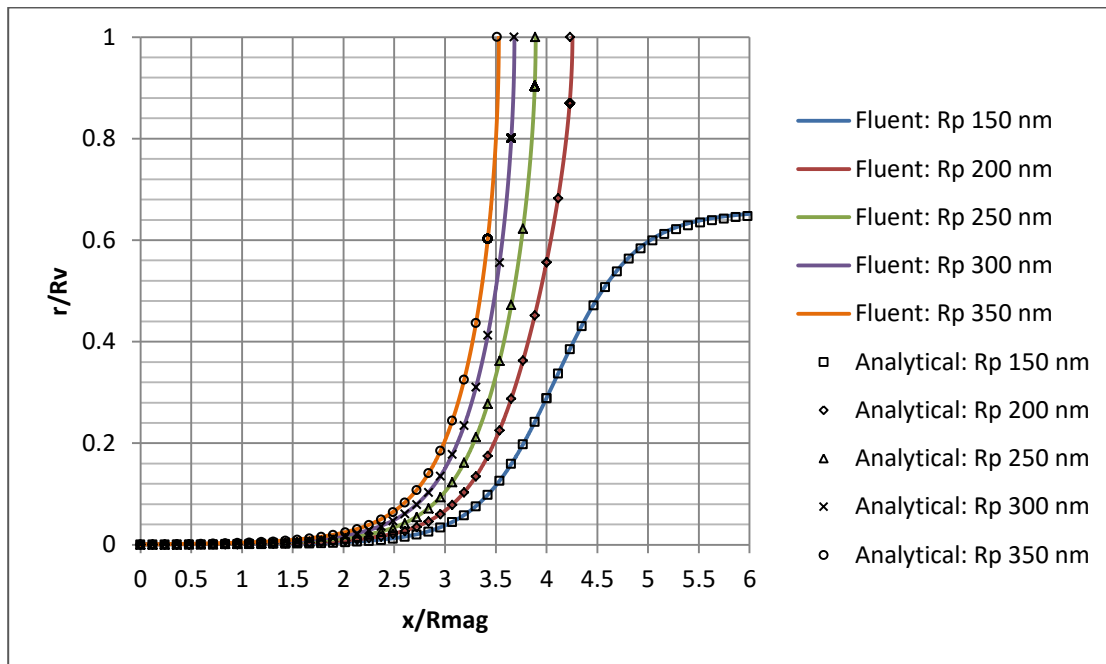


**Figure 6.** Trajectories for different particles radii for single injection case ( $y_{mag} = 0.025$  m).

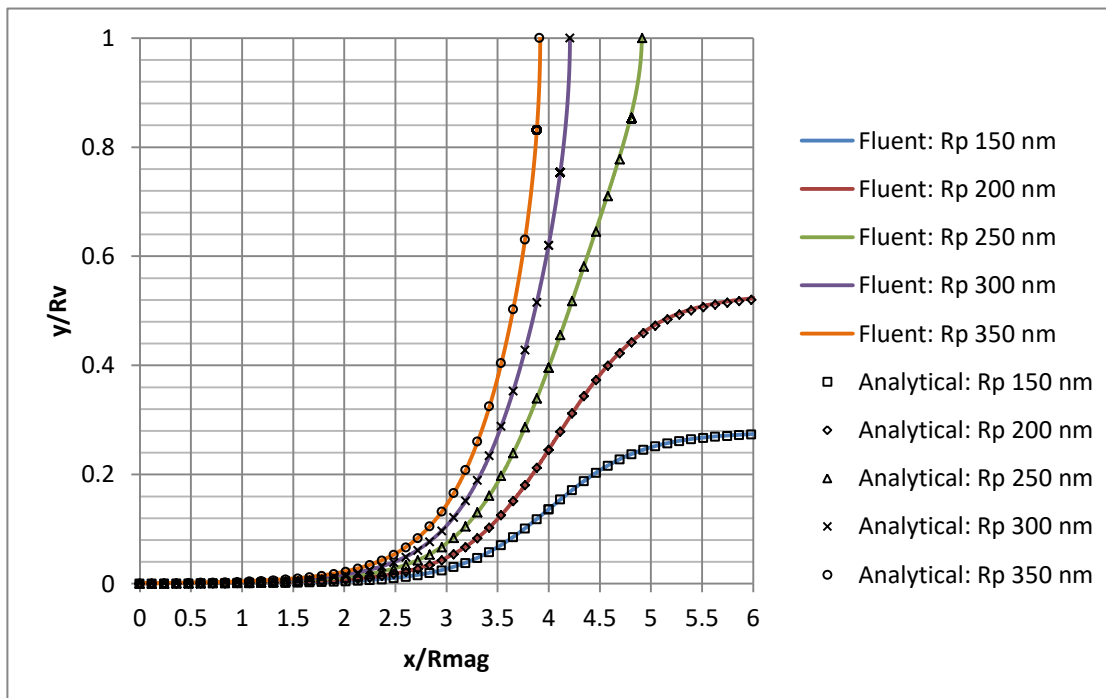


**Figure 7.** Trajectories for different particles radii for single injection case ( $y_{mag} = 0.030$  m).

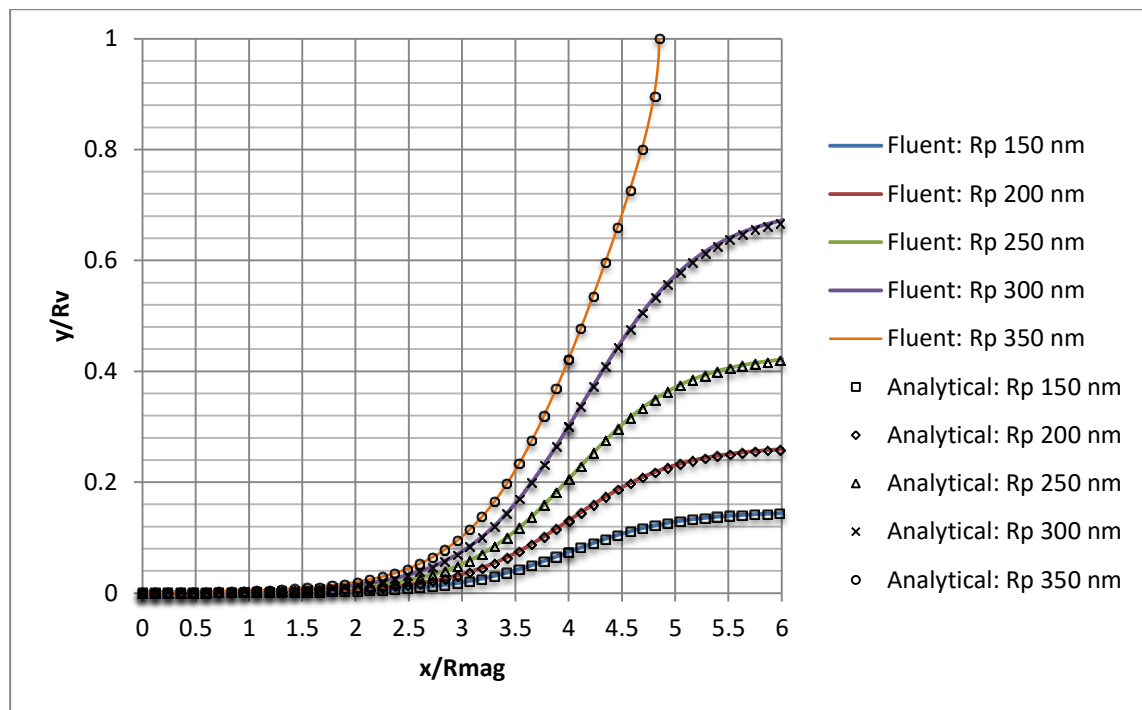


**Figure 8.** Trajectories for different particles radii for single injection case ( $y_{mag} = 0.035$  m).

### 3.3. Multipoint Injection Case

For this case, the two components of equation of motion of the particle in the equation (14) and equation (15) are being solved to observe their trajectories for  $y_{mag} = 0.035$  m. 19 particles for each radius of  $R_p$  for 150 nm, 200 nm, 250 nm, 300 nm and 350 nm are injected at the inlet. Next, the capture efficiency for each radius of the particle is calculated as shown in table 1.

From the five particles radii above, it is observed that the magnetic force is not symmetric. This is because, when the particles are injected closer to the external magnet (closer to the upper wall), it will go towards the left side position because of the higher value of magnetic force in both components of  $x$  and  $y$  there. Therefore, the particle will be captured more as it moves closer to the external magnet position. From the capture efficiency in table 1 below, it shows that the higher the particle radius, the higher the capture efficiency. It has been shown that the higher size of particle has the higher tendency to be captured by the external magnet because of the proportionality between the size of particle and magnetic force.

Furthermore, by simulating the particle trajectories using line injection method, the Region of Interest (ROI) of the particles can also be determined. As shown in figure 9, larger particle has larger and wider ROI because it has higher capture efficiency.

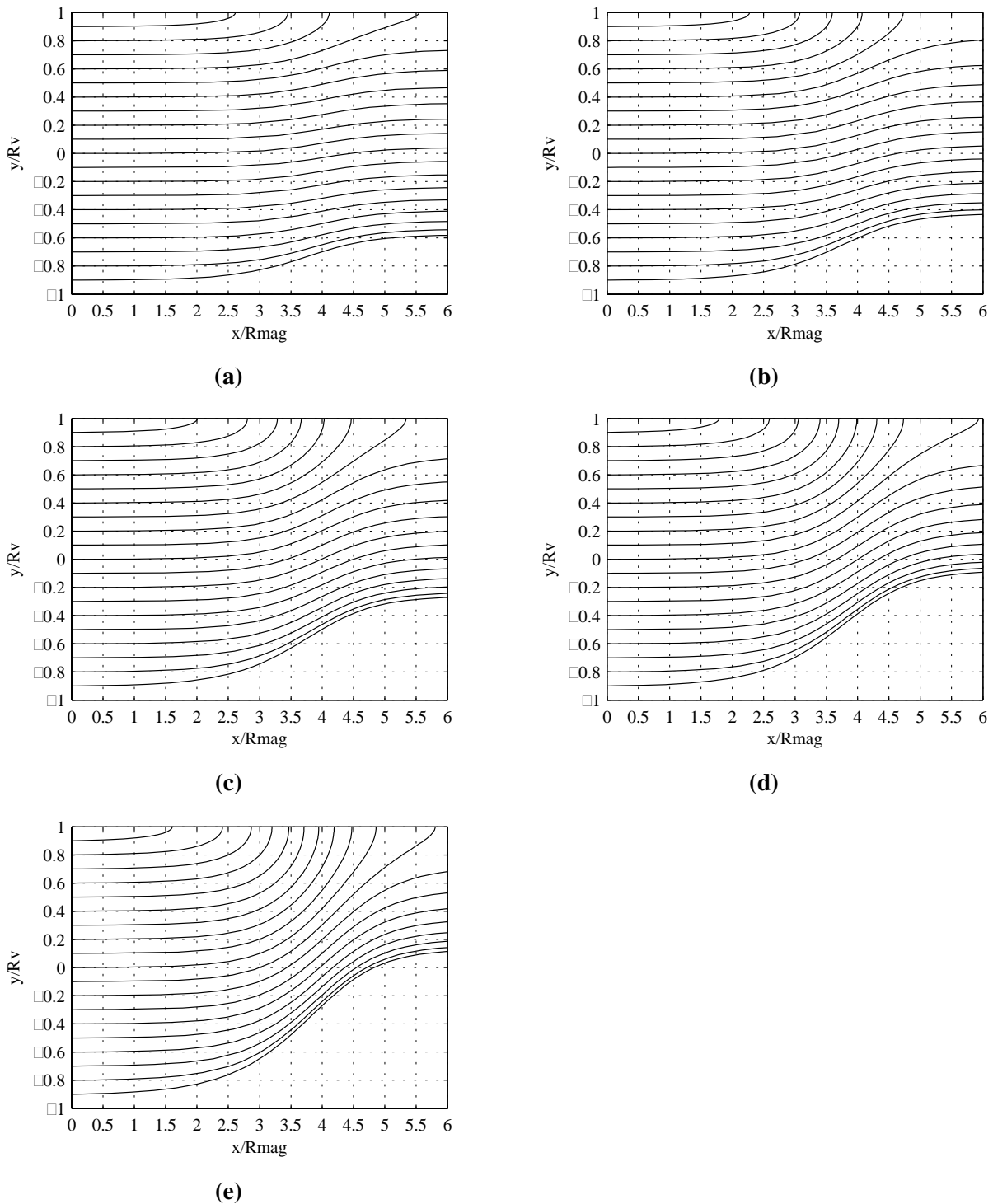


**Figure 9.** Trajectories for different particles radii for multipoint injection case at ( $y_{mag} = 0.035\text{m}$ ).

(a)  $R_p = 150\text{ nm}$ , (b)  $R_p = 200\text{ nm}$ , (c)  $R_p = 250\text{ nm}$ , (d)  $R_p = 300\text{ nm}$ , (e)  $R_p = 350\text{ nm}$ .

Table 1 Capture Efficiency for multipoint injection case.  
 (19 injected particles at inlet and  $y_{mag} = 0.035$  m)

Radius (nm)	Trapped	Escaped	Capture Efficiency
150	4	15	21 %
200	5	14	27 %
250	7	12	37 %
300	9	10	48 %
350	11	8	58 %

#### 4. Conclusion

In summary, the simulations using DPM ANSYS Fluent are successfully performed to study the effect on particle trajectories in microvessel when varying the particle radii and the external magnetic field locations. By only considering the dominant magnetic forces and fluid drag forces, it is found that the particle trajectories are strongly dependent on the particle size and the location of the external magnetic source. For single injection case, the minimum captured radius is  $R_p = 150$  nm, 250 nm, and 350 nm for  $y_{mag} = 0.025$  m, 0.030 m, and 0.035 m respectively. The simulation then can be used to determine the optimum particle size for magnetic drug targeting technique, given its size and location. Meanwhile, for multipoint injection, the capture efficiency is predicted for injected particles at  $y_{mag} = 0.035$  and it is increasing as the size of particle increases. The capture efficiency is 21%, 27%, 37%, 48% and 58% for  $R_p = 150$  nm, 200 nm, 250 nm, 300 nm, and 350 nm respectively.

It can be concluded that the concept of the minimum captured radius in single point injection is not valid for multipoint injection case. This is because there are particles will be captured even the radius of the particle is smaller than the minimum captured radius in multipoint injection case. Even for minimum captured radius, not all particles are captured since there are some particles lost because the injection points are everywhere through the inlet, not only at the centerline. However, the capture efficiency in multipoint injection will increase as the radius of the particle is close to the minimum captured radius in single injection point. At the end, this study can give some information about the size of the magnetic nanoparticles and the location of the magnetic field.

#### Acknowledgments

Authors gratefully thank Kuliyah of Engineering, International Islamic University Malaysia for financial support to publish this work.

#### References

- [1] Ramchand C, Pande P, Kopcansky P, Mehta R 2001 Application of magnetic fluids in medicine and biotechnology *Indian Journal of Pure and Applied Physics* **39**(10) pp 683– 686
- [2] Asmatulu R, Zalich M, Claus R, Riffle J 2005 Synthesis, characterization and targeting of biodegradable magnetic nanocomposite particles by external magnetic fields *J. Magn. Mag. Mater* **292** pp 108–119
- [3] Kayal S and Ramanujan R V 2010 Anti-cancer drug loaded Iron-Gold core-shel nanoparticles (Fe@Au) for magnetic drug targeting *J. Nanosci. Nanotechnol.* **10** pp 5527-5539
- [4] Mahmoudi M, Simchi A, Imani M, Milani A S and Stroeve P 2008 Optimal design and characterization of superparamagnetic iron oxide nanoparticles coated with polyvinyl alcohol for targeted delivery and imaging *Journal of Physical Chemistry B* **112** pp 14470-14481
- [5] Lee J, Isobe T and Senna M 1996 Preparation of ultrafine  $Fe_3O_4$  particles by precipitation in the presence of PVA at high PH *Journal of Colloid and Interface Science* **117** pp 490-494

- [6] Behrens S, Bonemann H, Matoussevitch N, Modrow H, Kempter V, Riehemann W, Wiedenmann A, Odenbach S, Will S, Eberbeck D, Hergt R, Landfester R K, Schmidt A, Schiller D, and Hempelmann R 2009 Synthesis and characterization *Colloidal Magnetic fluids: Basics, Development and application of Ferrofluids*, ed S Odenbach (Berlin: Springer-Verlag) chapter 1 pp 1- 69
- [7] Furlani EJ, Furlani E P 2007 A model for predicting magnetic targeting of multifunctional particles in the microvascular *J. Magn. Mag. Mater.* **312** pp 187–193
- [8] Aviles M O, Ebner A D and Ritter J A 2008 *In vitro* study of magnetic particle seeding for implant-assisted-magnetic drug targeting *J. Magn. Magn. Mater.* **320**(21) pp 2640-2646
- [9] Ritter J A, Ebner A D, Daniel K D, and Stewart K L 2004 Application of high gradient magnetic separation principles to magnetic drug targeting *J. Magn. Magn. Mater.* **280**(2) pp 184-201
- [10] Rotariu O and Strachan N J C 2005 Modelling magnetic carrier particle targeting in the tumor microvasculature for cancer treatment *J. Magn. Magn. Mater.* **293** pp 639-646
- [11] ANSYS® Academic Research, Release 15.0, Help System, Fluent Theory Guide, ANSYS, Inc.
- [12] ANSYS® Academic Research, Release 15.0, Help System, Fluent User's Guide, ANSYS, Inc.
- [13] Batchelor G K 1970 *An Introduction in Fluid Dynamics* (London: Cambridge University Press), p 233